Modelling the Spatial Forest-Thinning Planning Problem Considering Carbon Sequestration and Emissions

Wan-Yu Liu[1,*], Chun-Cheng Lin[2], and Ke-Hong Su[2]

[1] *Department of Forestry, National Chung Hsing University, Taichung 402, Taiwan*

[2] *Department of Industrial Engineering and Management, National Chiao Tung University, Hsinchu 300, Taiwan*

Abstract

Appropriate forest thinning is beneficial for growing forests and protecting ecological environments. To determine a beneficial approach in both economic and environmental aspects, carbon sequestration and emissions caused by forest-thinning activities can be traded. However, previous research on forest planning has not considered a detailed and sophisticated calculation for forest thinning and carbon sequestration. Hence, this study proposes a spatial forest-thinning planning problem involving carbon sequestration and emissions, which determine forest-thinning schedules over a planning period so that the total thinned timber volume over the period and the revenue from carbon sequestration and emissions can be maximized under certain spatial constraints. For this research, we first created a novel mathematical programming model, which can generally solve only small-scale problems. Therefore, this study also proposes an improved simulated annealing heuristic approach (ISA), which iteratively searches for a near optimal solution with two improved designs: a spatial local search operator and a neighborhood search scheme. The simulation results obtained using 300 forestland instances revealed that the proposed ISA can achieve better results through the proposed spatial local search operator, and run more efficiently through the proposed neighborhood search scheme. In addition, the decision regarding carbon sequestration and emissions was verified to be clearly advantageous for the cycling and sustainability of forest resources.

Keywords: Forest thinning, carbon sequestration, carbon trading, forest planning, simulated annealing, spatial planning

[*] Corresponding author. *E-mail address:* wyliu@nchu.edu.tw (Wan-Yu Liu)

1. Introduction

Forests are one of the most crucial ecological components in the earth's biosphere, playing a key role in reducing atmospheric CO_2 levels, providing habitat for animal communities, regulating hydrological turbulence, and protecting the soil. Forest planning includes numerous forest management activities; for instance, forest harvesting and renewal (Liu & Lin, 2015), forest conservation (avoiding excessive deforestation) (Fotakis, 2015), forest restoration (including afforestation and reforestation), forest tending, the management and usage of nonwood forest products in forests, and the establishment and tending management of urban forests. The forest planning in this study involves identifying a balance between economic and environmental benefits in forest harvesting. Forest harvesting or planning is generally characterized by a computationally complex mathematical model, because it concerns various economic and environmental factors, such as different management units and time periods, adjacency and green-up constraints associated to environmental objectives and regulations, the amount of timber to be harvested, whether the forestland is to be developed into a tourist area, the water supply, the range and size of the biological habitat, and ecological maintenance (Kazana et al., 2003; Arabatzis, 2010).

Forest planning includes temporal and spatial dimensions. Aside from the planning time period, the temporal dimension considered in recent studies has shifted to including the tree growth time (Myronidis & Arabatzis, 2009; Fotakis et al., 2012), because the model that considers the temporal dimensions of both planning periods and tree growth time is more complete. For the spatial dimension, the adjacency constraint (Wilkinson & Anderson, 1985; Murray, 1999; Kurttila, 2001) restricts two adjacent forest areas from being harvested concurrently. Note that the adjacency constraint considered in this study is the URM (unit restriction model) (Murray, 1999), and another frequently-used model is the area restriction model (ARM), which incorporates the construction of clusters from stands. In addition, the adjacency constraint usually involves with the green-up constraint (Nalle et al., 2005), which allows only the forests that grow for more than a minimum time period or until a certain tree height to be harvested. Forest-planning problems with various objectives and constraints have been modeled and solved using mathematical programming methods (Hoganson & Rose, 1984; Hof & Joyce, 1993; Borges & Hoganson, 1999). However, mathematical programming methods cannot mitigate large-scale problems because they are involved with integer varia-

bles so that they are generally computationally complex, i.e., they could not be solved efficiently by software on ordinary computers. Hence, various heuristic and metaheuristic approaches have been proposed; for instance, the nonsorting genetic algorithm II (Deb et al., 2002; Ducheyne et al., 2004, 2006), Monte Carlo integer programming (Boston & Bettinger, 1999), threshold accepting (Dueck & Scheuer, 1990), the great deluge algorithm (Dueck, 1993), the evolutionary algorithm (Liu et al., 2006; Mathey et al., 2007), simulated annealing (SA) (Ohman & Eriksson, 2002; Borges et al., 2014; Dong et al., 2015a), and the cultural algorithm (Liu & Lin, 2015). These approaches for forest planning generally adopt a scheme that circumvents local optimal solutions while searching for solutions. Among these approaches, SA has been shown to produce among the best solutions efficiently for some forest-planning problems with spatial concerns (Bettinger et al., 2002; Boston & Bettinger, 1999; Liu et al., 2006; Lockwood & Moore, 1993; Ohman & Eriksson, 2002; Ohman & Lamas, 2005).

Dong et al. (2015b) considered the forest-planning problem with carbon sequestration, in which the utility function consists of the harvested timber volume, carbon stocks, and spatial aggregation of the management activities. Their simulation considered forests of four ages (i.e., the actual, young, normal, and older), and the SA was applied to search for the maximal utility for forests at four ages. They found that the older forest landscape has the highest average utility value. Their work is of interest because it integrates the harvested timber volume, carbon stocks, and spatial aggregation of the management activities in a utility function. Note that these factors have been receiving much attention from ecological environmental and landscape aspects. The authors provided forest managers a comprehensive analysis to understand the performance of the three factors of different forest landscapes.

This study proposes a novel spatial forest-planning problem involving forest thinning and carbon trading, which have never been considered in previous research. These two concerns are respectively explained as follows:

Forest harvesting is further classified into clearcutting, thinning, and selective harvesting. Forest clearcutting involves nearly all trees in an area to be harvested being felled. The advantage of clearcutting is that it allows the convenience for mechanical logging by using large ground-based equipment (e.g., excavators), and does not require identifying the trees that should be felled. However, forest clearcutting could negatively impact the soil, with potentially harmful effects on sapling (young tree) growth, water conservation due to erosion,

the landscape, and animal dwellings. In addition, certain countries or areas do not allow any forest clearcutting (e.g., Taiwan). However, forest thinning involves the selective removal of trees. Generally, only trees that have achieved the standard to be cut (i.e., when some tree branches or stems impede the growing space of other trees) can be felled, whereas the others are left to grow. Selective harvesting also involves the selective removal of trees. The difference of selective harvesting from forest thinning is that the former harvests mature, overripe, and defective trees and reserves a sufficient number of healthy trees with commercial value; the latter moderately trims trees to tend trees and improve adjustment of growing space. Note that the method in this study can be applied to both thinning and selective harvesting under assumptions for problem simplification; only thinning is mentioned in the rest of this paper.

Appropriate forest thinning is beneficial, because it allows uncut trees to have more space to grow, so that more timber can be harvested (Assmann, 1970, 1961); the ecological environment can be protected (Beck, 1983; Haveri & Carey, 2000); forest resources can keep growing and be reused; and sustainable forest management can be achieved. Therefore, timber harvesting in some countries or regions involves forest thinning. However, to the best of our knowledge, conventional spatial forest-planning problems have not provided detailed and sophisticated calculation for forest thinning and carbon concerns.

Long-term forest planning should consider not only economic aspects but also ecological environments and social responsibility (Kangas & Kangas, 2005). Greenhouse gas (GHG) is one of the reasons for global warming. The main GHGs are water vapor (about 60-70%) and CO_2 (about 26%). Relatively speaking, humans are more able to control CO_2 emissions (from controlling the amount of human's burning fuels, deforestation, and biological respiration). Thus, CO_2 emissions receive a lot of attention, and are regarded as one of the major methods to mitigate global warming. Except for external forces (e.g., being absorbed by trees), atmospheric CO_2 levels are not easily reduced. As human activities are one of the reasons for CO_2 emissions, the amount of CO_2 emissions increase with a rising global population. Hence, certain green projects have been proposed for CO_2 adsorption (Hassall and Associates, 1999, p. 23), and have fostered an emerging carbon-trading market through which the sequestration and emissions of carbon are commodities that can be traded. Based on the Kyoto Protocol and the Paris Agreement, those countries that signed the agreements has a regulated yearly quota of CO_2 emissions, and will be encouraged if its carbon emissions do not exceed the

quota[†]. In the forest carbon-trading market, if forestland owners (sellers) afforest or reforest their land, they will obtain some quota of carbon sequestration (carbon certificates). When a firm (buyer) exceeds its regulated quota of CO_2 emissions, it can purchase the carbon sequestration quota from the sellers to offset its own insufficient quota to achieve the goal of reduction of carbon emissions. Thus, the sellers will obtain carbon benefits except for timber revenues. Conventional forest-planning problems rarely considered forest carbon trading. Recently, Dong et al. (2015b) have considered the forest planning problem with carbon sequestration. However, their work did not consider transforming carbon sequestration and emissions into the total net present value (NPV) to be traded, and did not focus on forest thinning.

This study proposes a spatial forest-planning problem that simultaneously considers forest thinning and carbon trading. Because a forestland is divided into multiple grids in which forests of each grid are assumed to be the same age (Borges et al., 2014), this problem involves determining a forest-thinning schedule for each year over a planning period (i.e., to determine the timber volume thinned in each grid at the end of each year), so that both the total harvested timber volume over the period and the revenue from carbon trading are maximized under the adjacency constraint (in which forests in two adjacent grids cannot be thinned concurrently) and the even timber flow constraint (in which the timber volume thinned this year must be no less than 90% and no greater than 110% of that thinned the previous year).

Note that the ratio of the timber harvested for heavily thinning achieves up to 36% (Štefančík & Bošeľa, 2014). If adjacent grids apply the heavily thinning, the wildlife and habitat could be destroyed. Therefore, this study considers the adjacency constraint for forest thinning. To simplify this problem, the number of treatment schedules (TSs) is assumed according to the analogy by Borges et al. (2014); each TS determines a timber volume thinned in each grid at the end of each year. Next, solving this problem involves identifying the TS applied in each forest grid. To address this problem, we first establish a mathematical programming model for it. Because SA has been shown to yield good performance in solving large-scale forest-planning problems (Bettinger et al., 2002; Boston & Bettinger, 1999; Liu et al., 2006; Lockwood & Moore, 1993; Ohman & Eriksson, 2002; Ohman & Lamas, 2005), we improve the SA to solve this problem. The main features of the proposed problem and approach are listed as follows:

- This study integrates the spatial forest-planning problem with a detailed and sophisti-

[†] UNFCC, Paris Agreement – Status of Ratification. Available at: http://unfccc.int/2860.php

cated mathematical formulation for forest thinning and carbon trading.

- Although the proposed SA approach is based on the SA approach for forest planning as detailed by Bettinger et al. (2002) and Borges et al. (2014), for iteratively improving a candidate solution, the proposed SA approach comprises two novel designs: (a) a spatial operator (Fotakis et al., 2012), which is a local search operator for improving the candidate solution if a certain forestland block adopts the same forest-thinning schedule as one of its adjacent forestland blocks; and (b) an approach avoiding searching repeated candidate solutions in the algorithm process to reduce the computing time in searching repetitive solutions.
- The proposed SA approach has a special design for generating the initial feasible solution to satisfy the adjacency constraint of the spatial forest-thinning problem.

Note that the main difference of this study from (Dong et al, 2015b) is that this study aims to identify a balance between the timber volume to be thinned and carbon emissions in a novel forest-thinning planning model.

The remainder of this study is organized as follows: Section 2 presents a description of the research problem and a basic introduction to SA. Section 3 describes the mathematical programming model targeting the research problem. Section 4 introduces the improved simulated annealing approach (ISA). Section 5 details our implementation of the proposed approach, and presents an experimental analysis for evaluating the performance of the proposed approach. Finally, Section 6 offers a conclusion and recommendations for future research.

2. Preliminaries

This section first details the research problem, and then introduces the legacy SA approach.

2.1 Problem description

Without loss of generality, consider a rectangular forestland consisting of N same-sized grids, called, "*management units*" (MUs), as shown in Figure 1(a), when $N = 9 \times 9$, and each MU has an area of 1 ha. An irregular forestland can also be applied; for problem simplification, we assume that the forestland was rectangular. Suppose that all trees in the forestland are of the same species; each MU has the same number of trees with the same age.

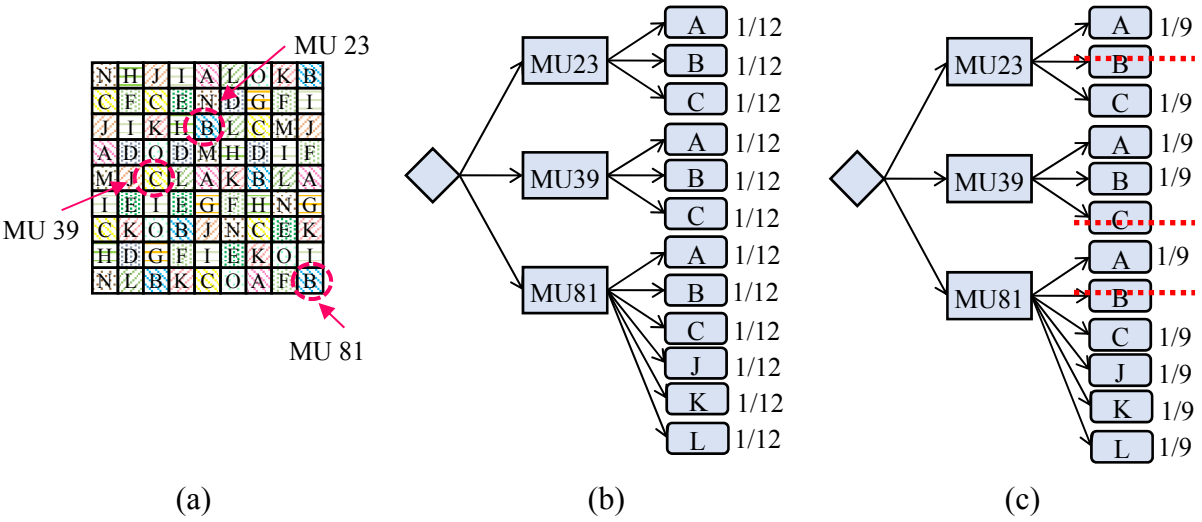

Figure 1. An example of selecting neighboring solutions. (a) A forestland with 9 × 9 MUs. (b) The decision tree of selecting neighboring states in (Borges et al., 2014). (c) The decision tree of selecting neighboring states in the proposed approach.

Consider a long-term planning period (say, T years). At the end of each year, each MU is assigned to *thinning treatment*, which is defined as the timber volume in this MU to be thinned. Hence, each MU must be assigned T thinning treatments over the T-year planning period, which are collectively referred to as a *treatment schedule* (TS) for this MU. For example, consider $T = 30$ planning years and 15 TSs (labeled A, B, …, O), as shown in Table 1. Each TS has 30 percentages, each of which represents the ratio of forests to be harvested through forest thinning at the end of the corresponding year. For example, in TS A, 16%, 26%, and 6% of the forests in this MU are respectively harvested at the end of Years 1, 6, and 11, whereas no forest in this MU is harvested in the other years for the first 13 years. Note that the time period between two harvests can be adjusted according to the practice.

Forest harvesting typically has an entry cycle for preventing excessive deforestation (e.g., the entry cycle in Table 1 is 5 years). With entry cycle R_a, all TSs can be categorized into R_a classes according to the years in which forest harvesting was conducted. For example, Table 1 lists an entry cycle of 5 years; hence, there are five TS classes: for $i = 1, 2, \ldots, 5$, each TS in class i harvests in the ith year of every 5 years. This classification is designed for satisfying the adjacency constraint, which can be avoided if two MUs are assigned TSs of different classes (i.e., if one of the two MUs is harvested in a certain year, then the other MU must not be harvested in that year because it is assigned a TS from a different TS class).

Table 1. An example with 15 TSs (divided into 5 classes) for a planning period of 30 years.

TS class	TS	Period (year)														
		1	2	3	4	5	6	7	8	9	10	11	12	13	…	30
1	A	16%	0	0	0	0	26%	0	0	0	0	6%	0	0	…	…
	B	16%	0	0	0	0	36%	0	0	0	0	16%	0	0	…	…
	C	26%	0	0	0	0	6%	0	0	0	0	6%	0	0	…	…
2	D	0	16%	0	0	0	0	26%	0	0	0	0	6%	0	…	…
	E	0	26%	0	0	0	0	6%	0	0	0	0	16%	0	…	…
	F	0	26%	0	0	0	0	6%	0	0	0	0	36%	0	…	…
3	G	0	0	16%	0	0	0	0	26%	0	0	0	0	6%	…	…
	H	0	0	6%	0	0	0	0	36%	0	0	0	0	16%	…	…
	I	0	0	26%	0	0	0	0	6%	0	0	0	0	36%	…	…
4	J	0	0	0	0.16	0	0	0	0	0.26	0	0	0	0	…	…
	K	0	0	0	0.26	0	0	0	0	0.06	0	0	0	0	…	…
	L	0	0	0	0.26	0	0	0	0	0.06	0	0	0	0	…	…
5	M	0	0	0	0	16%	0	0	0	0	26%	0	0	0	…	6%
	N	0	0	0	0	26%	0	0	0	0	6%	0	0	0	…	16%
	O	0	0	0	0	26%	0	0	0	0	6%	0	0	0	…	36%

Because environmental conditions and tree species in each MU may differ (e.g., plants in an MU may grow differently because of different geographical locations). Hence, different MUs should be assigned different TSs.

Based on these assumptions and settings, the spatial forest-thinning problem concerns determining a TS for each MU over a T-year planning period. In other words, a solution to this problem can be represented as an assignment of N TSs to N MUs, as shown in Figure 1(a), in which the letter attached to each MU is the label of the TS assigned to this MU. After the assignment of TSs to all MUs, the total net present value (NPV) of the total timber amount harvested per year (V_1), the cutting cost per year (V_2), and the penalty cost of carbon emission due to harvesting (V_3) can be calculated. In addition, after forest thinning per year, the revenue of carbon sequestration (V_4) increases for each year when the forests grow, except for being harvested at the end of this year. The V_3 and V_4 variables can be translated into a market value through carbon trading. Therefore, the objective of determining a TS for each MU over a T-year planning period is to maximize $V_1 + V_2 + V_3 + V_4$ under the following two constraints:

- *Adjacency constraint*: If two adjacent MUs share a common boundary or a common geographical point, they cannot be thinned concurrently for the preservation of wildlife habitat or ecological protection.
- *Even timber flow constraint*: The timber amount harvested each year must be no less than 90% and no greater than 110% of the timber amount harvested in the previous year. This constraint restricts declining and rising rates of the timber volume to be harvested,

so that the value of the capacity and investment activities are fixed when the capacity cost is assumed to be extremely high compared with the NPV (Allard et al., 1988).

The main differences of this problem compared with those addressed in past studies are that we also considered the NPVs of the carbon emission penalty cost and carbon sequestration revenue; and the treatment schedules for forest thinning differ from the previous forest planning model of (Borges et al., 2014). Moreover, the forest emission penalty cost occurs only at the end of each year, but the carbon sequestration revenue is recalculated for a complete year. Thus, integrating all of these considerations into the problem is challenging.

2.2 Legacy simulated annealing approach

SA (Kirkpatrick et al., 1983) is a metaheuristic algorithm that is used for identifying optimal solutions to combinatorial optimization problems, which can circumvent local optimal solutions by analogy, by simulating the annealing process of a solid. SA has been adopted for various applications in forest policy and economics; for instance, for estimating the supply of juniper biomass (Lauer et al., 2015) and assessing the impact of the Common Agricultural Policy on agriculture and forestry (Borges et al., 2010). The basic concept on which SA is based (Algorithm 1) concerns encoding a candidate solution of the research problem as a *state* of the solid (characterized by a string of parameters for determining the solution), and the objective function of the problem as an *energy level* of the state. Hence, the process of searching for an optimal solution to the research problem corresponds to the annealing process of identifying a solid state with the minimal energy level. Generally, the annealing process allows for only transferring the solid from its original state to a lower-energy *neighboring state* (i.e., a better neighboring solution), which is identical to the original state except for perturbation on certain parameters of the original state (Line 5 of Algorithm 1). Aside from transferring to a lower-energy neighboring state, the SA includes a temperature-cooling design presenting the state with the likelihood (Line 6) of transferring to a higher-energy neighboring state (i.e., a worse neighboring solution). In this design, the SA begins at a high temperature δ_h (Line 2 of Algorithm 1); hence, the solid has a high likelihood of transferring to a higher-energy neighboring state. Fixed at this temperature, this design enables identifying an optimal state of the solid after a fixed number of iterations; the state is called an *equilibrium state* at this temperature (Line 4 of Algorithm 1). Next, the SA iteratively cools down the solid (Line 10 of Algorithm 1) (i.e., the likelihood of transferring to a worse neighboring state diminishes), and finds its equilibrium state at a lower temperature. Until the SA achieves

the lowest temperature δ_l, the final state can have a minimal energy level. Finally, it is decoded as the final solution to the problem.

Algorithm 1 SA

Required: Set the highest temperature δ_h, and the lowest temperature δ_l

Generate an initial state x of the solid, and evaluate its energy $E(x)$
Let current temperature $\delta = \delta_h$
while $\delta \geq \delta_l$ **do**
    while the equilibrium state at temperature δ is not found **do**
        Find a neighboring state x' of state x via perturbation on state x, and evaluate its energy $E(x')$
        if $E(x') < E(x)$ or ($E(x') \geq E(x)$ and $rand(0, 1) < exp(-(E(x') - E(x))/(k_B \cdot \delta))$) **then**
            Replace x by x'
        end if
    end while
    Decrease temperature δ
end while
Decode state x as the final solution of the problem

3. The Proposed Mathematical Programming Method

By referring to the models by Borges et al. (2014) and Cacho et al. (2003), we create a mathematical programming model for the research problem. Because trees can be harvested only at the end of each of the T years, the end of the t-th year is called *key time t* throughout the remainder of this paper (i.e., T key times are considered). The notation used in this model is listed in Table 2. The decision variables of this model are as follows:

$$x_{ij} = \begin{cases} 1, & \text{if MU } i \text{ applies TS } j; \\ 0, & \text{otherwise.} \end{cases}$$

$$k_{jt} = \begin{cases} 1, & \text{if TS } j \text{ haversts a nonzero volume at key time } t; \\ 0, & \text{otherwise.} \end{cases}$$

The average tree age τ_{ij1} for each MU $i \in \{1, 2, \ldots, N\}$ and each TS $j \in M_i$ are provided. With these notations, the research problem involves determining a TS for each MU such that the NPV of the total revenue (including the profit from the harvested timber volume and the carbon revenue or penalty cost from carbon trading) of the forest-thinning scheduling is maximized under the constraints of adjacency and even timber flow. The mathematical programming model for this problem is expressed as follows:

$$\text{Maximize } Z = \sum_{i=1}^{N} \sum_{j=1}^{M_i} NPV_{ij} \cdot x_{ij} \tag{1}$$

s.t. $$\sum_{j=1}^{M_i} x_{ij} = 1, \quad \forall i \in \{1,2,...,N\} \tag{2}$$

$$VH_t = \sum_{i=1}^{N}\sum_{j=1}^{M_i} vh_{ijt} \cdot x_{ij}, \quad \forall t = 1,2,...,T \tag{3}$$

$$0.9 \cdot VH_{t-1} \le VH_t \le 1.1 \cdot VH_{t-1}, \quad \forall t = 2,3,...,T \tag{4}$$

$$vh_{ijt} = V(\tau_{ij(t-1)} + 1) \cdot \lambda_{jt}, \quad \forall i \in \{1,2,...,N\}, \quad \forall j \in M_i, \quad \forall t = 2,...,T \tag{5}$$

$$\tau_{ijt} = (V^{-1}(V(\tau_{ij(t-1)} + 1) - vh_{ijt})) \cdot k_{jt} + (\tau_{ij(t-1)} + 1) \cdot (1 - k_{jt}),$$

$$\forall i \in \{1,2,...,N\}, \quad \forall j \in M_i, \quad \forall t = 2,...,T \tag{6}$$

$$k_{jt} x_{ij} + k_{j't} x_{i'j'} \le 1, \quad \forall (i,i') \in I, \quad \forall (j,j') \in J, \quad \forall t = 1,2,...,T \tag{7}$$

$$x_{ij} \in \{0,1\}, \quad \forall i \in \{1,2,...,N\}, \quad \forall j \in M_i \tag{8}$$

$$k_{jt} \in \{0,1\}, \quad \forall j \in M_i, \quad \forall t = 1,2,...,T \tag{9}$$

Table 2. The notations used in this model.

Notation	Meaning	Unit
N	Number of MUs.	-
M_i	Set of TSs for MU i. Note that different MUs could apply different TSs, under constraints of the concerned problem.	-
NPV_{ij}	The NPV when MU i applies TS j.	$
VH_t	The total timber volume harvested at key time t.	m^3
vh_{ijt}	The total timber volume when MU i applies TS j at key time t.	m^3
T	Number of years of the planning period, i.e., number of key times.	-
I	The set including all pairs of adjacent MUs.	-
J	The set of each pair of TSs which are applied, respective, by each pair of adjacent MUs.	-
p_v	The coefficient of transforming timber volume into a market value, say the timber price.	$/$m^3$
$d(\tau)$	Average diameter of a tree at age τ.	m
τ_{ijt}	The average tree age projected when MU i applies TS j at key time t.	year
$V(\tau)$	The timber volume of a forest in which each tree is at age τ.	m^3
r	Discount rate.	-
$b(\tau)$	The total carbon stock for an MU in which each tree is at age τ.	tC/ha
υ	The coefficient of transforming carbon in tress into a CO_2 amount in atmosphere.	tCO_2/tC
p_b	The coefficient of transforming a CO_2 amount into a market value.	$/$tCO_2$
λ_{jt}	The percentage of the timber volume thinned in TS j at key time t.	-
$c_E(v)$	The cost of harvesting a timber volume v.	$

In this model, Objective (1) is to maximize the NPV of the total revenue of the for-

est-thinning scheduling (i.e., sum of NPV_{ij} when each MU i is assigned a certain TS j). Constraints (2) and (8) ensure that only one x_{ij} is equal to 1 (i.e., each MU must apply only one TS). Constraint (3) is used for calculating the total timber volume harvested at key time t to be the sum of the total timber volume when MU i is assigned a certain TS j at key time t. Constraint (4) concerns the even timber flow constraint (i.e., the timber amount VH_t harvested at each key time must be no less than 90% and no greater than 110% of the timber amount $VH_{t\text{-}1}$ harvested during its previous key time). Constraint (5) is used for computing the total timber volume vh_{ijt} when MU i is assigned TS j at key time t, which is nonzero only when the percentage λ_{jt} is nonzero. Constraints (6) is used for computing the average tree age τ_{ijt} projected after MU i is assigned TS j at key time t, which is either the projected age after harvesting or the age of the previous year + 1. Constraints (7) is the adjacency constraint (i.e., adjacent MUs cannot be harvested at the same key time). Constraints (8) and (9) fix the decision variables x_{ij} and k_{jt} as binary.

At the end of the forest-thinning planning in this study, the remaining forests are not clear-cut. Because each key time is the end of each year, the clearcutting at the last key time violates Constraints (4) and (7) (i.e., adjacency constraint and even timber flow constraint, respectively). In addition, even if clearcutting occurs at the last key time, a larger penalty for carbon emissions will be generated, so that we may not obtain a larger objective value.

In Objective (1), we modify the equation by Cacho et al. (2003) to compute NPV_{ij}, as follows:

$$NPV_{ij} = \sum_{t=1}^{T} vh_{ijt} \cdot p_v(d(\tau_{ijt})) \cdot (1+r)^{-t} - \sum_{t=1}^{T} c_E(vh_{ijt}) \cdot (1+r)^{-t}$$
$$+ \sum_{t=1}^{T} (b(\tau_{ijt}) - b(\tau_{ijt}-1)) \cdot \upsilon \cdot p_b \cdot (1+r)^{-t} - \sum_{t=1}^{T} b(V^{-1}(vh_{ijt})) \cdot \upsilon \cdot p_b \cdot (1+r)^{-t} \qquad (10)$$

On the right side of Equation (10), the first term represents the discounted market value of the timber volume harvested over T years, which is computed as follows: When MU i is assigned TS j at key time t, each sub-term in the sum is the harvested timber volume vh_{ijt}, times its timber price $p_v(d(\tau_{ijt}))$ (depending on the average diameter of the harvested trees at age τ_{ijt}) times its discount factor $(1 + r)^{-t}$. The second term represents the discounted timber cutting cost, in which the harvested timber volume vh_{ijt} results in a cutting cost $c_E(vh_{ijt})$. The third term is the discounted carbon sequestration revenue, in which each sub-term in the sum is the difference between carbon stocks at τ_{ijt} and $\tau_{ij(t-1)}$ (i.e., $b(\tau_{ijt}) - b(\tau_{ij(t-1)})$) multiplied by the

C-to-CO_2 transformation rate υ times the CO_2 price p_b times its discount factor $(1 + r)^{-t}$. The final term is the discounted carbon emission penalty cost, in which the projected age when the timber volume is vh_{ijt} and is calculated as $V^{-1}(vh_{ijt})$ years before it is substituted into the $b(.)$ function to determine the amount of carbon emissions, and is then transformed into a market value similarly.

In the first term in Equation (10), the timber price p_v for the harvested trees at age τ is linearly dependent on the average diameter $d(\tau)$ of the trees (Venn et al., 2000; Cacho et al., 2003), and is computed as follows:

$$p_v(d(\tau)) = \gamma_0 + \gamma_1 \cdot d(\tau); \tag{11}$$

$$d(\tau) = 200 \cdot \sqrt{\frac{a(\tau)}{\pi \cdot D}}; \tag{12}$$

where γ_0 and γ_1 represent the intercept and slope of the linear relation; D is the number of trees per hectare; and $a(\tau)$ is the area of the wood at age τ, and is computed as follows:

$$a(\tau) = \theta_a(1 - \exp(-\alpha_a \cdot \tau))^{\beta_a}; \tag{13}$$

where parameters θ_a, β_a, and α_a are determined according to tree species, environmental conditions, and forest management.

In the second term in Equation (10), $b(\tau)$ represents the total carbon stock for an MU in which each tree is at age τ, which is computed as follows:

$$b(\tau) = \phi \cdot [(\rho \cdot \theta_v)^{\mu} \cdot w(\tau)]^{1/1+\mu} \tag{14}$$

where parameters ϕ, ρ, θ_v, and μ are determined according to tree species, environmental conditions, and forest management; and $w(\tau)$ depicts the carbon stock in stemwood biomass for an MU in which each tree is at age τ, and is computed as follows:

$$w(\tau) = \rho \cdot V(\tau) \tag{15}$$

where parameter ρ is determined according to tree species; and $V(\tau)$ is the timber volume of a forest in which all trees are at age τ, and is computed as follows:

$$V(\tau) = \theta_v[1 - \exp(-\alpha_v \cdot \tau)]^{\beta_v} \tag{16}$$

where parameters θ_v, β_v, and α_v are determined according to tree species, environmental conditions, and forest management.

In the third term in Equation (10), the forest-cutting cost $c_E(vh_{ijt})$ is computed as follows:

$$c_E(vh_{ijt}) = c_f + c_v \cdot vh_{ijt} \tag{17}$$

where c_f is the fixed cost; and c_v represents the variable cost for each cubic meter of timber harvested at each key time.

In the fourth term in Equation (10), with timber volume v, the projected tree age is computed as follows:

$$\tau = V^{-1}(v) = \frac{-\ln(1-\exp((\ln v - \ln \theta_v)/\beta_v))}{\alpha_v} \tag{18}$$

Equation (18) is derived from the inverse function of $V(\tau)$ in Equation (16).

The differences of the proposed model from those presented in past studies (e.g., Borges et al., 2014; Cacho et al., 2003) involve Equations (5), (6), (7), (9), (10), (17), and (18). These differences which are explained as follows:

- Past research has not provided an explanation into how to compute vh_{ijt} (by estimating the remaining timber volume after thinning) compared with this study, which addresses this with Constraint (5).
- Because the previous model in (Borges et al., 2014) had not considered modeling the forest-thinning problem, they were not required to compute the tree age after forest thinning, but we do so with Constraints (6) and (9).
- The adjacency constraint in the Borges et al. (2014) study is based on the assumption that if one MU is determined to be harvested, then its adjacent MUs are not harvested for the entire T-year planning period. Rather than the entire period, we considered the adjacency constraint for each key time (i.e., although one MU harvested at this key time renders the harvesting of its adjacent MUs forbidden at this key time, these adjacent MUs can be harvested at other key times, as characterized in Constraints (7), (8), and (9). Note that key times have been addressed in the literature as green-up constraints (Nalle et al., 2005; Borges et al., 2014).

- Cacho et al. (2003) considered the NPV from carbon sequestration and emission for only a forest entry cycle. By contrast, we extend their research by computing the NPV for *T*-year planning periods in Equation (10).

In addition, this study has the following features, though some previous works may also have these features. Different from Cacho et al. (2003) that considered a fixed forest-cutting or establishment cost, we extend it to include the sum of the fixed and variable costs in Equation (17). Different from Cacho et al. (2003) that provided only the formula of the timber volume of a forest in which all trees are at age τ, we used Equation (18) to estimate a tree age after forest thinning.

4. Proposed Improved SA Approach

This study proposes the ISA, as shown in Algorithm 2 and Figure 2, for addressing the problem detailed in Section 3. The ISA has two improved designs: (a) a spatial local search operator (Line 6 in Algorithm 2); and (b) the circumvention of identifying the same state in searching neighboring states (Line 7 in Algorithm 2) for increasing the efficiency of the algorithm. The ISA is detailed in Algorithm 2, and is explained as follows:

Initially, the ISA requires setting two parameters to initialize a temperature-cooling scheme: highest temperature δ_h and lowest temperature δ_l. Next, the ISA generates an initial state x of the solid using Algorithm 3 (Line 1), and evaluates its fitness $f(x)$ using Algorithm 4 (Line 2). When the current temperature δ is set to the highest temperature δ_h (Line 3), the ISA enters a nested repetitive loop (Lines 4 – 14), in which the outer while loop repetitively executes the inner while loop (Lines 5 – 12) and lowers the current temperature δ by multiplying it by a scaling factor T_s between 0 and 1 (Line 13) until the current temperature δ is lower than the lowest temperature δ_l (Line 4). The inner while loop (Lines 5 – 12) repetitively adjusts state x by using the proposed spatial local search operator in Algorithm 5 (Line 6), identifies a new neighboring state x' according to the proposed new neighborhood search scheme in Algorithm 6 (Line 7), evaluates the fitness $f(x')$ of state x' (Line 8), and determines whether to replace state x with state x' (Line 10) according to the criteria expressed in Line 9 until the solid finally achieves an equilibrium state at temperature δ (i.e., the state remains barely unchanged in the previous *TE* iterations) (Line 5).

Algorithm 2 ISA

Required: Set highest temperature δ_h, and lowest temperature δ_l

Generate a feasible initial state x of the solid by Algorithm 3
Evaluate fitness $f(x)$ of state x by Algorithm 4
Let current temperature $\delta = \delta_h$
while $\delta \geq \delta_l$ or the maximal iteration NI is not achieved **do**
    while the equilibrium state at temperature δ is not found **do**
        Adjust state x using a spatial local search operator in Algorithm 5
        Find a new neighboring state x' according to a new scheme in Algorithm 6
        Evaluate fitness $f(x')$ of state x' by Algorithm 4
        if $f(x') > f(x)$ or ($f(x') \leq f(x)$ and $rand(0, 1) < exp(-(f(x) - f(x'))/(k_B \cdot \delta))$) **then**
            Replace x by x'
        end if
    end while
    Decrease temperature δ, i.e., $\delta = T_s \times \delta$
end while
Decode state x as the final solution of the problem

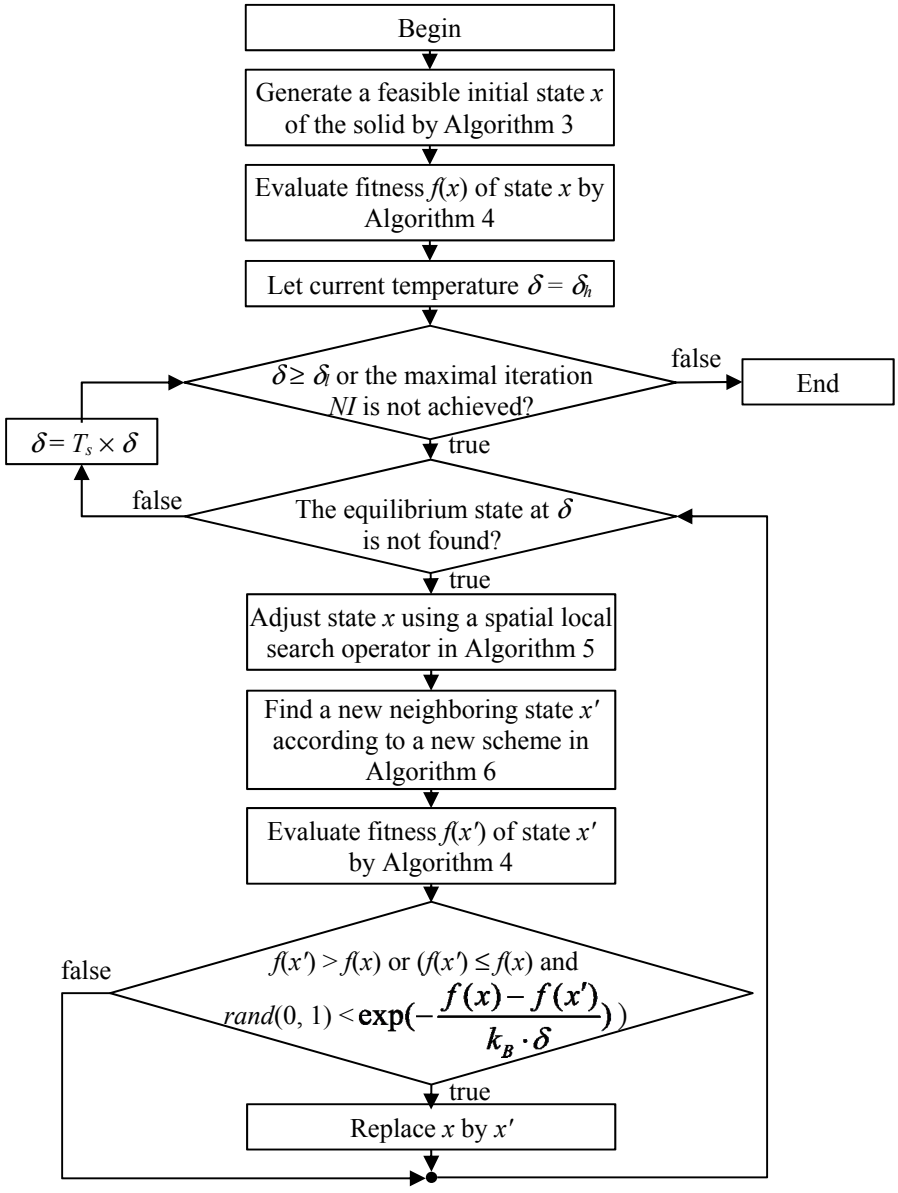

Figure 2. Flowchart of Algorithm 2.

The main two improved designs include the spatial local search operator for adjusting state x (Line 6) and the new neighborhood search scheme for determining the neighboring state x' (Line 7). The main components of designing the ISA are detailed in the remainder of this section.

4.1 Solution encoding

The first step to design the ISA to solve the research problem is to encode a candidate solution for the problem as a state (i.e., a string of parameters). Consider a forestland divided into $N = n \times n$ MUs as shown in Figure 1(a). For $i, j \in \{1, 2, \ldots, n\}$, the MU at the i-th row and the j-th column is called the $((i - 1) \times n + j)$-th MU. For each $i \in \{1, 2, \ldots, N\}$, the i-th MU can be assigned M_i TSs. With this notation, a state of the ISA is represented as a vector $(y_1, y_2, \ldots, y_N)$ where each $y_i \in \{1, 2, \ldots, M_i\}$ is the label of the TS assigned to the i-th MU for each $i \in \{1, 2, \ldots, N\}$.

4.2 State initialization

Because in this study we considered adjacency and even timber flow constraints, no all states correspond to feasible solutions. The proposed ISA is designed to initiate in a feasible initial state that satisfies the adjacency constraint. Therefore, this subsection presents Algorithm 3 for generating such a feasible state, and Figure 3 is the flowchart of Algorithm 3.

Algorithm 3 INITIALIZE A STATE

Required: Remind that R_a-year entry cycle leads to R_a classes of TSs. It is required that $R_a \geq 4$.

1: Randomly select four classes of TSs, renamed classes 1, 2, 3, and 4
2: Consider four patterns of shaded MUs in the forestland (e.g., an example for 10×10 MUs is shown in Figure 4(a)-(d))
3: **for** $i = 1$ to 4 **do**
4: Each shaded MU in pattern i is assigned with a random TS in class i
5: **end for**
6: Randomly select L_c MUs, and change these MUs to be assigned with TSs in the other classes (different from the selected four classes)

As mentioned in Subsection 2.1, R_a-year forest entry cycle leads to R_a classes of TSs (e.g., $R_a = 5$ in Table 1). Line 1 of Algorithm 3 randomly selects four of those TS classes and relabels them Classes 1, 2, 3, and 4. Next, Line 2 considers four patterns of shaded MUs in the forestland (An example involving 10×10 MUs is shown in Figures 2(a)–(d)). For $i = 1, .., 4$, each shaded MU in pattern i is assigned with a random TS in class i, as shown in Figure 4(e). Thus far, the state corresponding to this assignment has been feasible for adjacency constraint because adjacent MUs are assigned two TSs from different classes that did not harvest forests

at the same key time. However, such a state occurs too frequently. To further diversify this feasible state, Line 6 randomly selects L_c MUs and modifies them to be assigned the TSs in the other classes (different from the four selected classes). This initial state satisfies only Constraints (2), (3), (5), (6), and (7), and may still violate Constraint (4) (i.e., the even timber flow constraint). Hence, Constraint (4) is penalized in the fitness function introduced later.

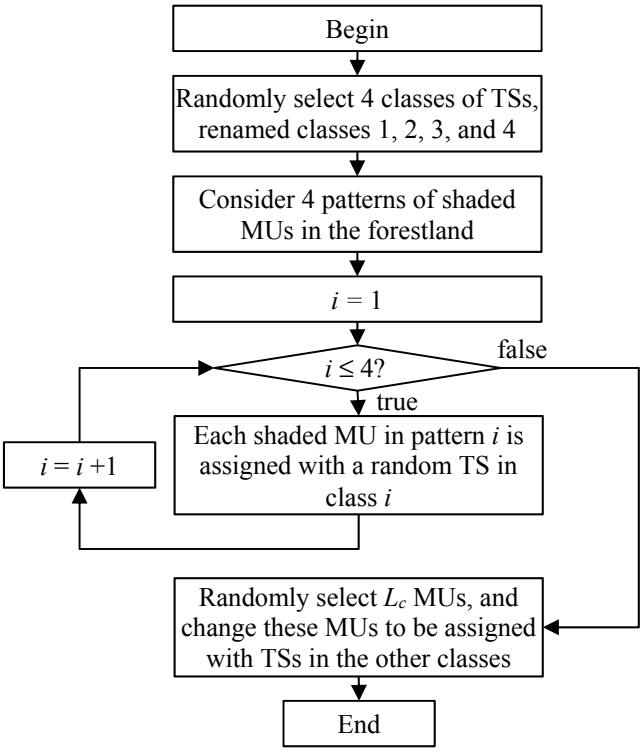

Figure 3. Flowchart of Algorithm 3.

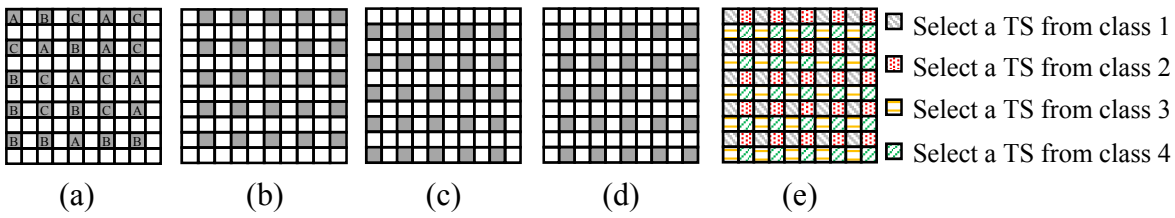

Figure 4. (a)-(d) An example of the four patterns of shaded MUs for a forestland with 10×10 MUs, in which the TSs from class 1 in Table 1 are assigned to the shaded MUs in (a). (e) Illustration of assigning the TSs from four TS classes to the four patterns.

Note that the concerned forest thinning model is implemented with TSs consisting of the ratios of the timber to be thinned at each time (e.g., see Table 1). One may think that the tim-

ber flow constraint can easily be addressed just by referring these ratios. In fact, however, the harvested timber volume at each key time is determined by not only numbers of these ratios but also the tree age at that key time. Hence, it would not be possible to just refer these ratios to address the timber flow constraint. In addition, the design of these ratios can be applied to both forest thinning and selection cutting.

4.3 State decoding and fitness evaluation

To evaluate the performance of a state, the state must be decoded as a solution for the research problem; next, a fitness value for this solution is calculated. In legacy SA, an energy level is typically used for evaluating the performance of a state for a minimization problem. However, because the research problem is a maximization problem, a fitness is used (i.e., a higher fitness of the state implies improved performance for its corresponding solution).

With state ($y_1, y_2, \ldots, y_N$), MU i is assigned TS y_i for each $i \in \{1, \ldots, N\}$. Next, we obtain the percentage $\lambda_{y_i t}$ of the timber volume thinned in each TS y_i at each key time t. Thus, the state can be decoded to compute its fitness $f(y_1, y_2, \ldots, y_N) = Z$ using Equations (1) and (10). However, in the proposed approach, the state must satisfy Constraint (2), (3), (5), (6), and (7), but may violates Constraint (4). Hence, the equation for evaluating the fitness of state (y_1, $y_2, \ldots, y_N$) is given as follows:

$$f(y_1, y_2, \ldots, y_N) = Z - \varphi^2 \tag{19}$$

where Z is Objective (1) of the research problem; and φ represents the penalty cost function for Constraint (4), and is computed as follows:

$$\varphi = \left(\sum_{t=1}^{T} | VH_t - VH_{t-1} |\right)^2 \tag{20}$$

where VH_t represents the total timber volume harvested at key time t. When $\varphi = 0$, the fitness function is equal to the objective function. Algorithm 4 is used for evaluating the fitness, and Figure 5 is the flowchart of Algorithm 4.

Algorithm 4 FITNESS_EVALUATION
Input: A state ($y_1, y_2, \ldots, y_N$)
Output: Fitness $f(y_1, y_2, \ldots, y_N)$ of this state

1: Let τ_i denote the age of wood of the i-th MU for $i = 1, 2, \ldots, N$
2: $Z = 0$
3: **for** $t = 1$ to T **do**

4: $VH_t = tmp = 0$
5: **for** $i = 1$ to N **do**
6: $tmp = tmp + (b(\tau_i + 1) - b(\tau_i)) \cdot \upsilon \cdot p_b$
7: $vh_{iy_i t} = V(\tau_i + 1) \cdot \lambda_{y_i t}$
8: $VH_t = VH_t + vh_{iy_i t}$
9: **if** $vh_{iy_i t} > 0$ **then**
10: $tmp = tmp + vh_{iy_i t} \cdot p_v(d(\tau_i + 1)) - c_E(vh_{iy_i t}) - (b(\tau_i + 1) - b(V^{-1}(V(\tau_i + 1) - vh_{iy_i t})) \cdot \upsilon \cdot p_b$
11: $\tau_i = \tau_i + V^{-1}(V(\tau_i + 1) - vh_{iy_i t})$
12: **else**
13: $\tau_i = \tau_i + 1$
14: **end if**
15: **end for**
16: $Z = Z + tmp \cdot (1 + r)^{-t}$
17: **end for**
18: **for** $t = 2$ to T **do**
19: **if** $|VH_t - VH_{t-1}| > 0.1 \cdot VH_{t-1}$ **then**
20: $\varphi = \varphi + |VH_t - VH_{t-1}|$
21: **end if**
22: **end for**
23: Output $f(y_1, y_2, \ldots, y_N) = Z - \varphi^2$

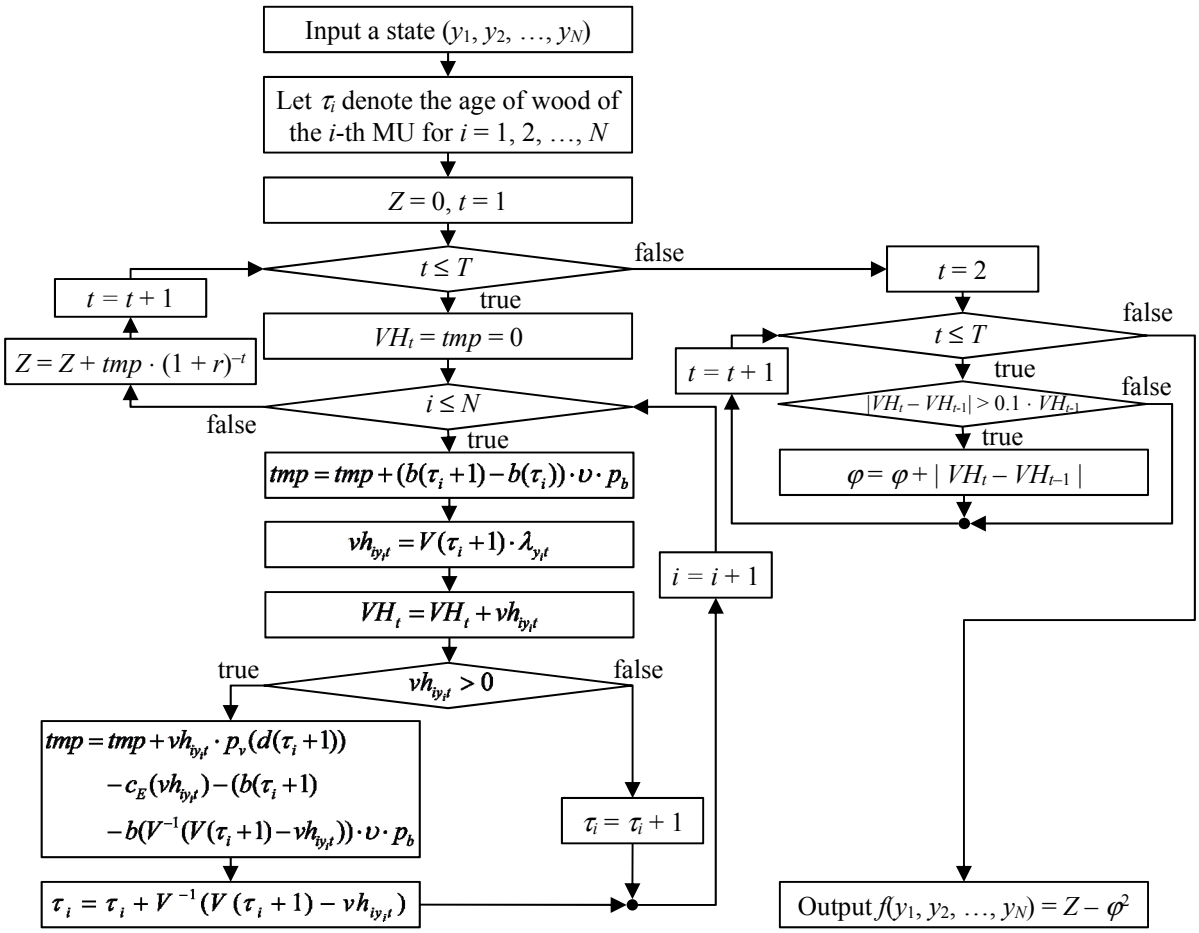

Figure 5. Flowchart of Algorithm 4.

4.4 Spatial local search operator

The research problem concerns a spatial consideration; hence a spatial local search operator (Fotakis et al., 2012) could improve efficiency of the algorithm. Therefore, in the proposed ISA, each iteration conducts a spatial local search operator on the current state x (Line 6 of Algorithm 2). The spatial local search operator functions based on the notation of forcing a number of MUs to be assigned the same TS with its 'proximal' MU, because proximal MUs have similar ecological geographical conditions; thus, they might be assigned the same TS in the optimal solution. Note that the so-called 'proximal' MUs of some MU i are the eight closest MUs in the same age class with MU i. For instance, in Figure 6(a), the MUs with labels are of the same age class. Consider the nine labeled MUs within the dotted circle in Figure 6(a). Then, the eight labeled MUs (i.e., labeled by 'J', 'A', 'O', 'C', 'B', 'A', 'C', and 'K') along the dotted circle contour are the 'proximal' MU of the center MU labeled by 'B'.

Algorithm 5 is the proposed spatial local search operator, which is explained as follows. First, Line 1 selects an MU (e.g., the i-th MU) in the forestland (e.g., to select the center MU of the dotted circle shown in Figure 6(a)). Next, Line 2 considers eight 'proximal' MUs (i.e., eight closest MUs under the adjacency constraint, except for the center MU in the dotted circle shown in Figure 6(a)). Thus, the output state does not violate Constraints (2), (3), (5), (6), and (7). In addition, the proposed spatial local search operator differs from that proposed by Fotakis et al. (2012) in selecting a proximal MU. Next, Line 3 then conducts a tournament selection to select one of the eight proximal MUs. Next, Line 4 considers a state x' that is identical to state x, except that the i-th MU is assigned the same TS that is associated with the selected proximal MU (Figure 6(b)). Finally, in Line 5, if fitness $f(x')$ of state x' is greater than fitness $f(x)$ of state x, then state x is replaced with state x'.

Algorithm 5 SPATIAL_OPERATOR

Input: The current state x.
Output: The adjusted state x.

1: Randomly select an MU, say the i-th MU, in the forestland
2: Consider 8 'proximal' MUs as shown in Figure 6(a)
3: Conduct tournament selection to select one of the 8 proximal MUs
4: Consider a state x' which is almost the same as state x except the i-th MU is assigned with the same TS associated with the selected proximal MU
5: If $f(x') > f(x)$, then x is replaced with by x'

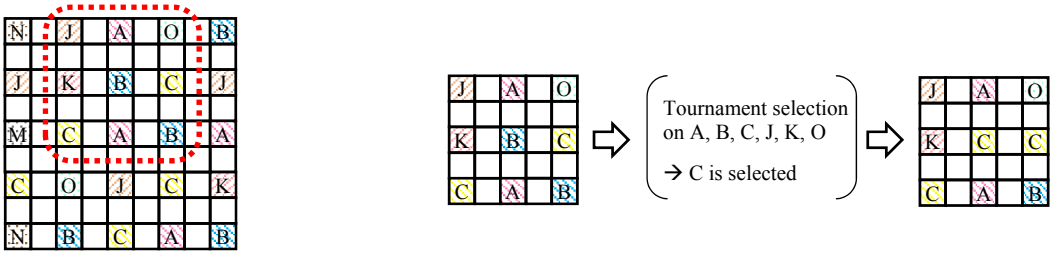

(a) (b)

Figure 6. An example of conducting the proposed spatial local search operator. (a) Randomly select an MU, i.e., the center of the dotted circle. (b) Conduct tournament selection to select one of the 8 proximal MUs, and let the center MU apply the same TS with the selected proximal MU.

4.5 New neighborhood search scheme

To solve a spatial forest-planning problem, Borges et al. (2014) proposed an SA algorithm with three neighborhood search schemes. The best of the three schemes is explained as follows. Consider the forestland consisting of 9 × 9 MUs displayed in Figure 1(a) as an example; as shown in the figure, the letter attached to each MU represents the TS applied to this MU. First, their scheme randomly selects three MUs before constructing a decision tree based on them. As shown in Figure 1(b), the root node of the decision tree is connected to the nodes associated with the selected three MUs, and the child nodes of each MU node represents the labels of all the feasible TS of the MU (i.e., those that satisfy the adjacency constraint). Next, their scheme randomly selects 1 of the 12 feasible terminal nodes with an equal likelihood 1/12. Finally, their scheme generates a neighboring state x' that is identical to state x, except that the MU with a child that is the selected terminal node of the decision tree is modified, so that the TS represented by this terminal node can be applied.

As shown in Figure 1(b), the previous Borges et al. scheme can generate a neighboring state x' that is identical to the original state x when the selected MU is assigned the original TS. For instance, as shown in Figure 1(b), MU 23 is assigned TS B; MU39 applies TS C; and MU 81 applies TS B. This leads to a computational inefficiency in their scheme solving the research problem. Hence, to solve this problem, in the current study, we remove the probabilities for selecting those inefficient TSs, as shown in Figure 1(c). Thus, the likelihood of selecting one of the other TSs becomes 1/9. Algorithm 6 details this neighboring state selection. Although this scheme is simple, each iteration of the main loop of the algorithm conducts this

selection once; hence, it has a considerable influences after executing a high number of iterations. Moreover, this scheme retains the feasibility of the neighboring state for the adjacency constraint, because the TSs of all terminal nodes are feasible.

Note that the proposed neighborhood search scheme that avoids unavailable solutions is often made in the previous literature on heuristics, and its performance depends on the problem being addressed. Fortunately, this scheme is suitable for addressing the problem concerned in this study.

Algorithm 6 SEARCH_A_NEIGHBOR

Input: The current state x.
Output: The neighboring state x'.

1: Randomly select three MUs in the forestland
2: Consider a decision tree in which the root node has three children corresponding to the three selected MUs; each of the three selected MUs has multiple leaf nodes each of which is corresponding to a feasible TS for this MU (i.e., not violating any constraints); and each leaf node has an equal probability to be selected
3: Randomly select a leaf node of the decision tree
4: Output a state x' which is almost the same as state x except the selected MU (i.e., the parent node of the selected leaf node) is assigned with the TS associated with this selected leaf node

To evaluate the performance of the proposed algorithm, the experiments conducted for this study involved simulating 300 artificial forestlands by referring to the experimental setting in the Borges et al. (2014) study. The 300 forestlands are divided into three tree-age classes (i.e., young, normal, and old), in which each forestland in the young-age class (resp., old-age class) has more young MUs (resp., old MUs); each forestland in the normal-age class has an equal number of young and old MUs (Table 3). Each forestland has an area of 1600 ha, and is divided into 40×40 MUs.

The parameters used in Equation (10) are listed in Tables 4 and 5. The data shown in Table 4 is based on the conditions of the terrain, environment, and rainfalls in South-eastern Australia and the tree species of Eucalyptus nitens (commonly known as Shining Gum) (Wong et al., 2000), which was applied in the simulation performed by Cacho et al. (2003). Table 5 lists the basic parameters used in the model.

Table 3. Distribution of age classes for different forest landscapes (Borges et al., 2014).

Age class (year)	Young	Normal	Old
[0,10]	15%	7.69%	1%
[11,20]	14%	7.69%	2%
[21,30]	13%	7.69%	3%
[31,40]	12%	7.69%	4%
[41,50]	10%	7.69%	5%
[51,60]	8%	7.69%	6%
[61,70]	7%	7.75%	7%
[71,80]	6%	7.69%	8%
[81,90]	5%	7.69%	10%
[91,100]	4%	7.69%	12%
[101,110]	3%	7.69%	13%
[111,120]	2%	7.69%	14%
≥ 121	1%	7.69%	15%

Table 4. Tree parameters and forest site characteristics (Wong et al., 2000).

Variable	Value
Tree parameters	
θ_v	262.956
α_v	0.252
β_v	4.651
θ_a	30.124
α_a	0.383
β_a	5.000
Forest site characteristics	
Site code	EP205
Location	Mount Gambier, SA
Date planted	July 1988
Previous land use	Pasture
Annual rainfall (mm)	766
Average temperature (°C)	
January	11.4–23.7
July	5.1–12.9
Annual pan evaporation (mm)	1262
Slope	Gentle
Altitude (m)	60
Soil type	Structured, clay loam

Table 5. The basic parameters used in the model by Cacho et al. (2003).

Parameter	Value	Unit	Reference
γ_0	-4.342	$	f
γ_1	0.936	$/cm	g
p_b	20	$/t	a
r	6	%	e
v	3.67	t CO_2/t C	b
D	250	trees/ha	g
ρ	0.378	t C/m^3	c
ϕ	1.429	*	d
μ	0.2	*	d
c_f	200	$	-
c_v	5	$	-

* No unit. Sources: a) Hassall and Associates (1999). b) Based on molecular weights of CO_2 and Carbon. c) Estimated as wood density. Carbon content of biomass = 0.7 (t/m3). 0.54; d) Calculated from parameters presented by Kirschbaum (2000). e) Arbitrary value subject to sensitivity analysis. f) Linear approximation to assumed data following Cacho et al. (2003). g) Assumed value following Cacho et al. (2003).

4.6 Parameter setting of the proposed ISA

This subsection presents a comparative analysis of the parameter settings of the proposed ISA (i.e., Algorithm 2), including the maximal number of iterations of the main loop of the ISA (*NI*), the number of iterations for the equilibrium state (*TE*), the highest temperature (T_h), the scaling factor for lowering temperature (T_s), the entry cycle length R_a, and the number of MUs to be changed in the initialization (L_c) used in Algorithm 3. We randomly selected one of the 300 forestland instances to analyze the effects resulting from adjusting these parameters. The selected forestland was the ninth forestland in the young-age class. In addition, only the feasible output solutions (i.e., $\varphi = 0$) were applied in this analysis for correctness.

For comparison against the proposed ISA, the SA approach without the proposed spatial local search operator and the new neighborhood search scheme was called *legacy SA*, and is the method for comparison throughout the remainder of this paper. The legacy SA approach can also be regarded as a variant of the approach used by Borges et al. (2014).

5. Simulation Results and Discussion

This section details the implementation of the proposed ISA for addressing the research problem. First, the experimental environment is described. Next, we detail our determination of the parameter setting, achieved after numerous experimental trials. Finally, a comprehensive analysis of the experimental results is provided.

5.1 Experimental environment

First, we conducted an experimental comparison with NI = 6,000, 8,000, 10,000, and 12,000. The plots of fitness versus the number of iterations in the ISA and legacy SA are displayed in Figures 7(a) and 7(b), respectively, in which the NI = 10000 case is shown to have the highest fitness for both approaches. The figures also show that each case has a different curve length because it converges (i.e., fitness has changed within 5% of its previous fitness value for the previous 30 iterations) at the end-point of its corresponding curve. Hence, we observed that both approaches converge in all cases. Similarly, the plots for the different settings of TE, T_h, T_s, R_a, and L_c using both approaches are given in Figures 7(c) and 7(d), Figures 7(e) and 7(f), Figures 7(g) and 7(h), Figure 8, and Figure 9. Analyzing these experimental results revealed that the best performance was achieved with the following settings: TE = 50, T_h = 10000, T_s = 0.99, R_a = 5, and L_c = 400 (Table 6); and both approaches converged in all cases.

5.2 Analyzing the fitness results and computing time

Since this study does not develop the global optimum or mixed integer solution, the assessments of heuristic results in this section are a Level 3 (of 6) validation process as described in (Bettinger et al., 2002). With the parameter settings mentioned in the previous subsections, we conducted an experimental analysis on 100 forestland instances of each of the three age classes (i.e., young, normal, and old) by using the ISA and legacy SA, and the boxplots of the fitness values of their experimental results are displayed in Figure 10. The medians for the young-age class in using the ISA and legacy SA were \$7,365,082 and \$6,610,339, respectively (Figure 10(a)). Note that all the currency throughout this paper is US\$. Those for the normal-age class in using the ISA and legacy SA were \$6,816,549 and \$6,082,754, respectively (Figure 10(b)). Those for the old-age class in using the ISA and legacy SA were \$6,295,892 and \$5,492,949, respectively (Figure 10(c)). As shown in Figure 10, the performance of the proposed ISA was superior to that of the legacy SA for all age classes.

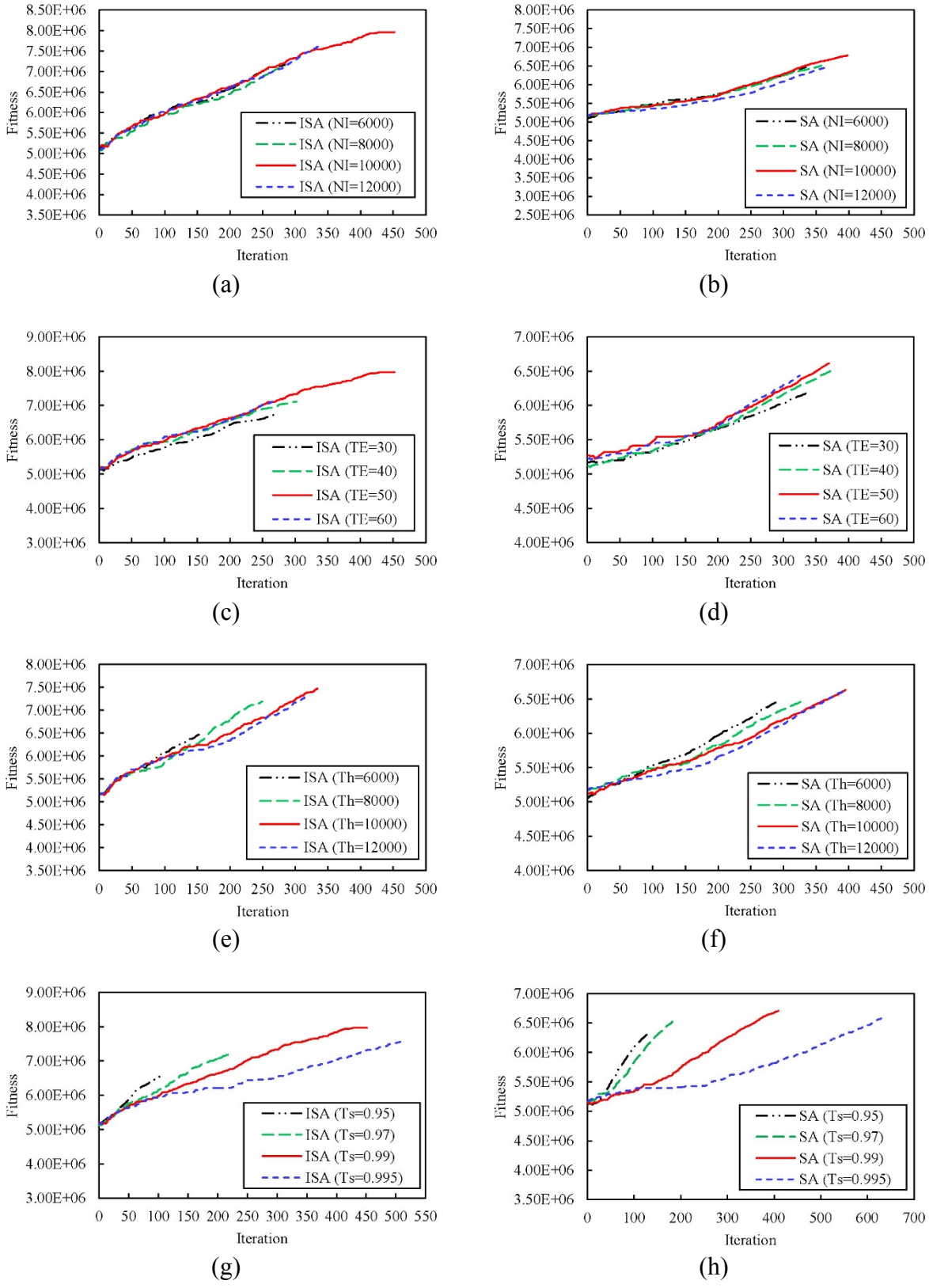

Figure 7. Experimental comparison using the ImSA and legacy SA under different parameter settings of (a)(b) *NI*, (c)(d) *TE*, (e)(f) T_h, and (g)(h) T_s.

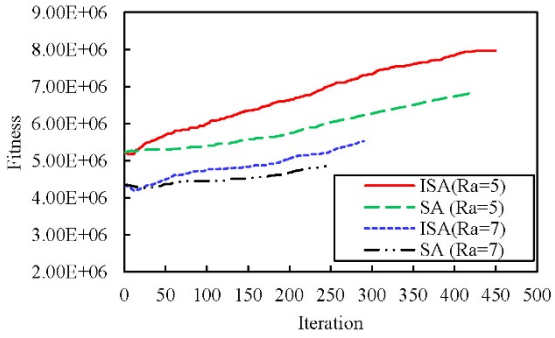

Figure 8. Experimental comparison using the ISA and legacy SA under different parameter settings of R_a.

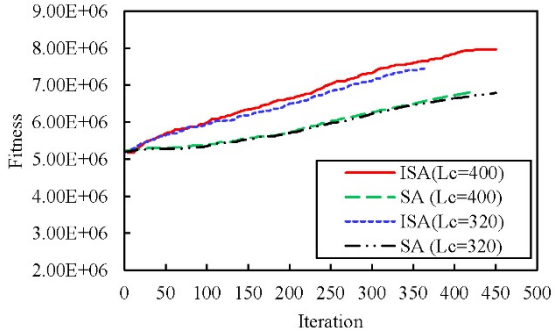

Figure 9. Experimental comparison using the ISA and legacy SA under different parameter settings of L_c.

Table 6. The parameter settings used in the proposed ISA.

Parameter	Value
Maximal number of iterations (*NI*)	10000
Number of iterations for equilibrium state (*TE*)	50
Highest temperature (T_h)	10000
Scaling factor for decreasing temperature (T_s)	0.99
Rotation period length (R_a)	5
number of MUs to be changed in initialization used in Algorithm 3 (L_c)	400

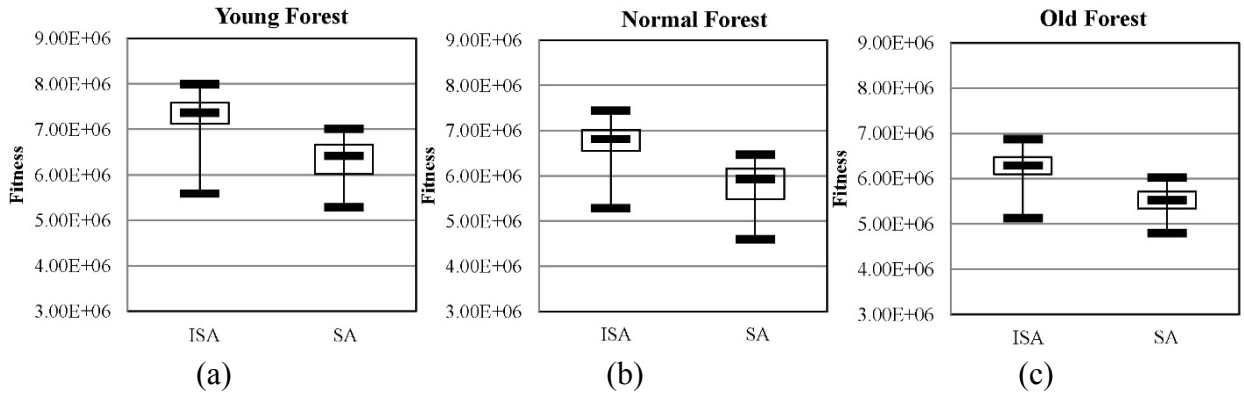

Figure 10. The boxplots of the fitness of the experimental results by using the ISA and legacy SA for three age classes.

The boxplots of the computing time when the ISA and legacy SA were used for the three age classes are shown in Figure 11. The medians for the young-age class in using the ISA and legacy SA were 2,637.481 s and 1,061.714 s, respectively (Figure 11(a)). Those for the normal-age class in using the ISA and legacy SA were 2601.138 s and 1070.44 s, respectively (Figure 11(b)). Those for the old-age class in using the ISA and legacy SA were 2591.045 s and 1018.931 s, respectively (Figure 11(c)). As shown in Figure 11, the ISA requires more computing time compared with legacy SA for all age classes.

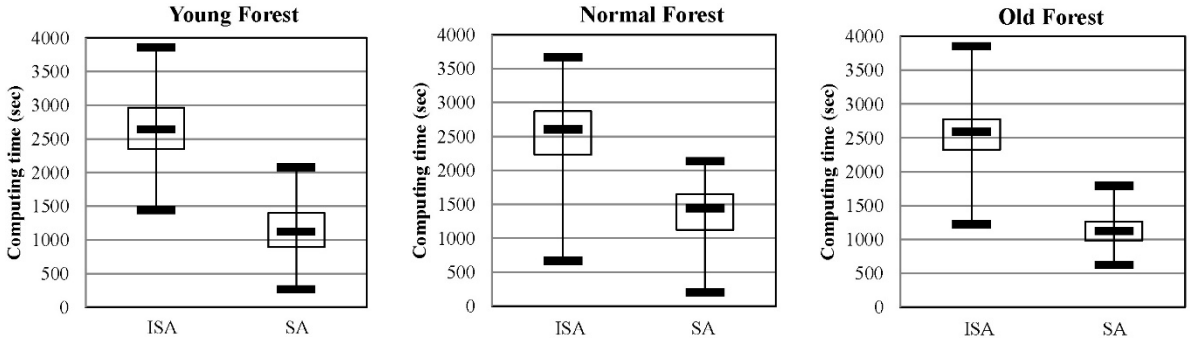

(a) (b) (c)

Figure 11. The boxplots of the computing time by using the ISA and legacy SA for three age classes.

The P values from Wilcoxon signed-rank tests for fitness and computing time between the ISA and legacy SA, with a 99% confidence level, are listed in Table 7. As shown in the table, all P values were less than 0.01, indicating significant differences between the fitness results (resp., computing time) obtained using the ISA and legacy SA for all age classes. Therefore, we speculated that the ISA requires more computing time but obtains better fitness results compared with SA.

Table 7. The P values from Wilcoxon signed-rank tests for the fitness and the computing time between the ISA and legacy SA.

Age class	The P value for fitness results	The P value for computing time
Young	2.716×10^{-29}	1.897×10^{-25}
Normal	2.834×10^{-20}	2.970×10^{-21}
Old	1.948×10^{-29}	4.809×10^{-34}

5.4 Analyzing the new neighborhood search scheme and the spatial local search operator

The ISA (i.e., SA with two improved designs: a new neighborhood search scheme and a spatial local search operator) can generate better fitness results compared with legacy SA. Hence, we further attempted to identify which of the two improved designs contributed more to performance. We considered the following four methods, which are combinations of the two designs: the ISA, SA with only the spatial local search operator (SASpaOper), SA with only the new neighborhood search scheme (SANNebor), and legacy SA. The four methods were used for each of the three-age classes 100 times, and their boxplots are shown in Figure 12. As displayed in the figure, because the fitness results of SASpaOper were superior to those of SANNebor in all the age classes, we speculated that the spatial local search operator was the main factor affecting performance of the ISA; however, the results of SANNebor were only a minor improvement over those of legacy SA.

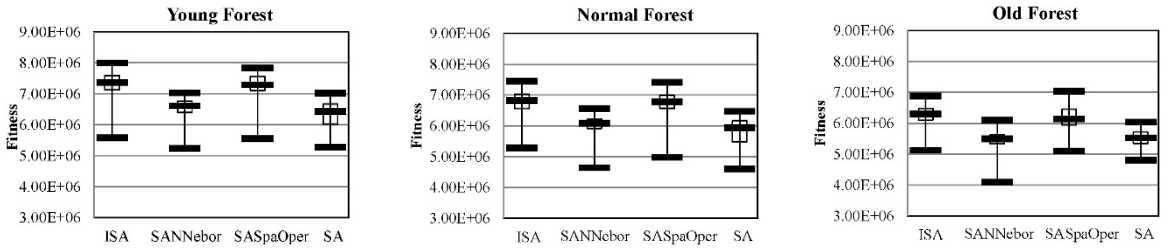

(a) (b) (c)

Figure 12. The boxplots of the fitness results of four methods for the three age classes.

A similar analysis was conducted for computing time (Figure 13). As shown in Figure 13, SANNebor ran faster than the other three methods did, including legacy SA; however, it still obtained better fitness results compared with legacy SA (Figure 12). In addition, the ISA (with the new neighborhood search scheme and spatial local search operator) ran faster than SASpaOper did (with only the spatial local operator). Therefore, we speculated that the proposed neighborhood search scheme was useful for increasing the computational efficiency of the ISA.

Furthermore, the convergence of the four methods was analyzed. Similarly, the ninth forestland from the young-age class was selected as a representative experimental instance. The plots of the fitness results versus the number of iterations for the four methods are shown in Figure 14, through which all methods can converge; and the ISA obtained the best fitness results.

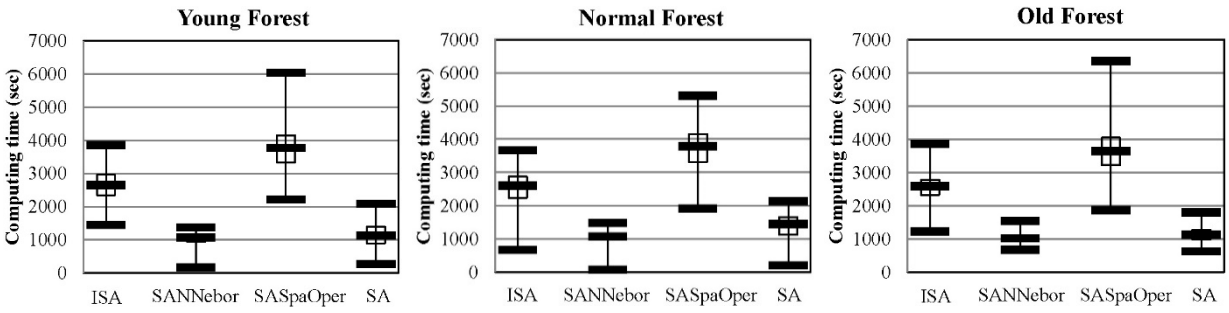

Figure 13. The boxplots of computing time of four methods for the three age classes.

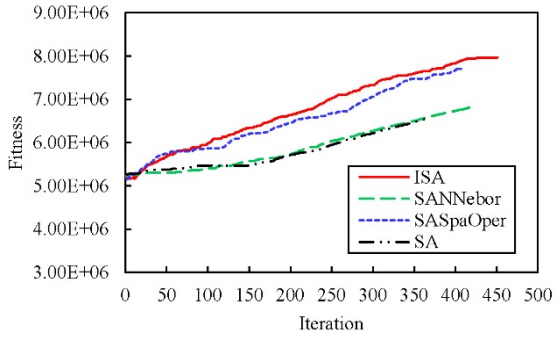

Figure 14. Comparison of convergence of four method.

The Wilcoxon signed-rank test results for each pair of fitness results and the computing time of the four methods for the three age classes are shown in Table 8. As listed in the table, in all the age classes, the fitness results obtained using the ISA (Method 1) differed significantly from those obtained using SANNebor (Method 2) but did not with those obtained using SASpaOper (Method 3). In other words, the spatial local search operator contributed more to the fitness performance of the ISA than did the new neighborhood search scheme. Hence, we speculated that the spatial local search operator was the main factor affecting the fitness performance of the ISA. Regarding computing time, the ISA (Method 1) differed significantly from SASpaOper (Method 3). In conclusion, we speculated that the ISA obtained good fitness results because of the spatial local search operator, and ran efficiently because of the new neighborhood search scheme.

Table 8. The P values from Wilcoxon signed-rank test for the fitness results and the computing of four methods.

Forest age class	Methods compared *	The P value for fitness results	The P value for computing time
Young	1 vs 2	1.018×10^{-28} **	8.793×10^{-26} **
	1 vs 3	6.949×10^{-1}	3.715×10^{-19} **
	1 vs 4	2.716×10^{-29} **	1.897×10^{-25} **
	2 vs 3	2.134×10^{-31} **	8.793×10^{-26} **
	2 vs 4	7.904×10^{-18} **	5.306×10^{-1}
	3 vs 4	2.664×10^{-32} **	8.793×10^{-26} **
Normal	1 vs 2	1.595×10^{-18} **	2.090×10^{-23} **
	1 vs 3	9.688×10^{-1}	2.970×10^{-21} **
	1 vs 4	2.834×10^{-20} **	2.969×10^{-21} **
	2 vs 3	3.083×10^{-21} **	1.874×10^{-25} **
	2 vs 4	9.570×10^{-4} **	1.127×10^{-8} **
	3 vs 4	1.260×10^{-22} **	2.210×10^{-25} **
Old	1 vs 2	1.971×10^{-20} **	1.177×10^{-23} **
	1 vs 3	9.948×10^{-1}	1.229×10^{-16} **
	1 vs 4	5.215×10^{-20} **	2.274×10^{-23} **
	2 vs 3	1.201×10^{-18} **	8.266×10^{-24} **
	2 vs 4	6.152×10^{-1}	2.168×10^{-4} **
	3 vs 4	7.782×10^{-15} **	8.266×10^{-24} **

* Method 1: ISA; Method 2: SANNebor; Method 3: SASpaOper; Method 4: legacy SA.
** P value < 0.001.

5.5 Analyzing cases with and without carbon trading

In addition to method improvement, one major feature of this study was the consideration of carbon trading in the problem setting. Therefore, this subsection presents an experimental comparison between the cases with and without carbon trading. Similarly, the ninth forestland of the young-age class is used as the experimental instance, and the plots of the experimental fitness results versus the number of iterations are displayed in Figure 15. From this figure, although the case with carbon trading converges for a longer time due to its complex computation, the final fitness result of the cases with carbon trading is better than the other case.

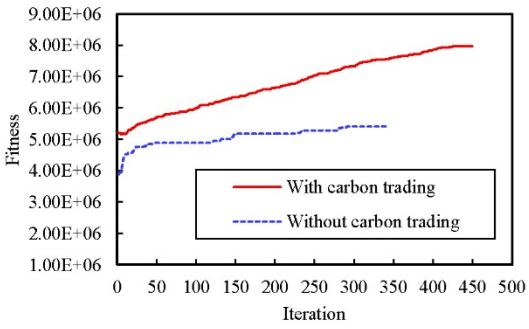

Figure 15. Comparison between the cases with and without carbon trading.

In what follows, we conduct experimental comparison between the cases with and without carbon trading on 100 forestland instances of each of the three age classes (i.e., young, normal, and old) by using ISA, and the boxplots of the fitness values of their experimental results are displayed in Figure 16. The medians for the young-age class in using the ISA are \$7,365,082 and \$6,047,748 in the cases with and without carbon trading, respectively (Figure 16(a)). Those for the normal-age class in using ISA are \$6,816,549 and \$6,145,711 in the cases with and without carbon trading, respectively (Figure 16(b)). Those for the old-age class in using ISA and legacy SA are \$6,295,892 and \$5,427,799 in the cases with and without carbon trading, respectively (Figure 16(c)). As shown in this figure, the case with carbon trading performs better than the other case.

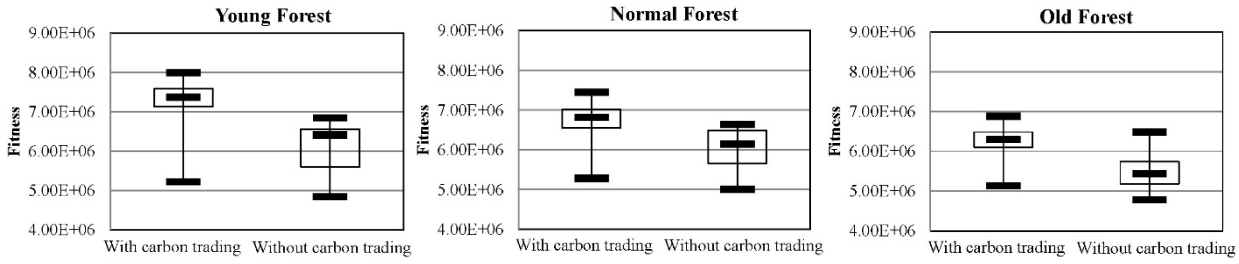

(a) (b) (c)

Figure 16. Boxplots of fitness of the experimental results between the cases with and without carbon trading for three age classes.

The P values from Wilcoxon signed-rank tests for fitness using the ISA between the cases with and without carbon trading, with a 99% confidence level, are listed in Table 9. As shown in this table, all P values are less than 0.01, indicating significant differences between the fitness results using the ISA between the two cases. Therefore, we speculated that the case with carbon trading obtains better fitness results than the case without carbon trading.

In light of the above, the case with carbon trading is preferred, because it not only has a better fitness (revenue) but also inspires environmental protection and could help slow down global warming. The mechanism of carbon sequestration revenue and carbon emission penalty can specify forestland owners in appropriate forest thinning or harvesting, to achieve cycling and sustainability of forest resources. If the carbon price can be promoted, the effect could be further amplified.

Table 9. The P values from Wilcoxon signed-rank tests for the fitness between the cases with and without carbon trading.

Age class	The P value for fitness results
Young	6.916×10^{-7}
Normal	1.104×10^{-5}
Old	1.794×10^{-4}

5.6 Future challenges

In the future, one line of future research could be to consider additional aspects regarding the conservation of soil, water, and wildlife in forest-thinning problems, because those aspects have a substantial impact on the global ecology. Another line of future research could involve implementing the proposed approach in a more complete forest model to establish conditions that are more practical, because the original appearance of a forest is highly complex and a forest includes multiple-species.

6 Conclusion

To achieve a balance between economic and environmental objectives and achieve sustainability in forest planning, this study has proposed a spatial forest-planning problem that considers forest thinning and carbon trading (through which carbon sequestration and emissions can be traded). To address this problem, we first modeled it as a mathematical programming model, and further proposed an ISA, which includes the designs of a new neighborhood search scheme and a spatial local search operator. The simulation and statistical results obtained from 300 artificial forestlands of three forest age classes revealed that the performance of the ISA was considerably superior to that of legacy SA. Furthermore, the results evidenced that the ISA obtained good fitness results because of the spatial local search operator, and ran efficiently through the new neighborhood search scheme.

Acknowledgements

This work has been supported in part by MOST 104-2221-E-009-101, Taiwan.

References

Allard, J., Errico, D., Reed, W. J., 1988. Irreversible investment and optimal forest exploitation. Natural Resource Modeling 2, 581–597.

Arabatzis, G., 2010. Development of Greek forestry in the framework of European Union policies. Journal of Environmental Protection and Ecology 11(2), 682–692.

Assmann, E., 1970. The Principles of Forest Yield Study: Studies in the Organic Production, Structure, Increment and Yield of Forest Stands. Pergamonn Press, Oxford, p. 506.

Assmann, E., 1961. Waldertragskunde: Organische Produktion, Struktur, Zuwachs und Ertrag von Waldbeständen. BLV Verlagsgesellschaft, München, p. 490.

Beck, D.E., 1983. Thinning increases forage production in Southern Appalachian Cove Hardwoods. Southern Journal of Applied Forestry 7, 53–57.

Bettinger, P., Graetz, D., Boston, K., Sessions, J., Chung, W., 2002. Eight heuristic planning techniques applied to three increasingly difficult wildlife planning problems. Silva Fennica 36(2), 561–584.

Borges, P., Eid, T., Bergseng, E., 2014. Applying simulated annealing using different methods for the neighborhood search in forest planning problems. European Journal of Operational Research 233, 700–710.

Borges, P. J., Fragoso, R., Garcia-Gonzalo, J., Borges, J. G., Marques, S., Lucas, M. R., 2010. Assessing impacts of Common Agricultural Policy changes on regional land use patterns with a decision support system: An application in Southern Portugal. Forest Policy and Economics 12(2), 111–120.

Borges, J.G., Hoganson, H.M., 1999. Assessing the impact of management unit design and adjacency constraints on forestwide spatial conditions and timber revenues. Canadian Journal of Forest Research 29, 1764–1774.

Boston, K., Bettinger, P., 1999. An analysis of Monte Carlo integer programming, simulated annealing, and Tabu search heuristics for solving spatial harvest scheduling problems. Forest Science 45(2), 292–301.

Cacho, O.J., Hean, R.L., Wise, R.M., 2003. Carbon-accounting methods and reforestation incentives. Australian Journal of Agricultural and Resource Economics 47(2), 153–179.

Deb, K., Pratap, A., Agarwal, S., Meyarivan, T., 2002. A fast and elitist multiobjective ge-

netic algorithm: NSGA-II. IEEE Transactions on Evolutionary Computation 6(2), 182–197.

Dong, L., Bettinger, P., Liu, Z., Qin, Z., 2015a. A comparison of a neighborhood search technique for forest spatial harvest scheduling problems: A case study of the simulated annealing algorithm. Forest Ecology and Management 356, 124–135.

Dong, L., Bettinger, P., Liu, Z., Qin, Z., 2015b. Spatial Forest Harvest Scheduling for Areas Involving Carbon and Timber Management Goals. Forests 6(4), 1362–1379.

Ducheyne, E., De Wulf, R.R., De Baets, B., 2004. Single versus multiple objective genetic algorithms for solving the even-flow forest management problem. Forest Ecology and Management 201, 259–273.

Ducheyne, E.I., De Wulf, R.R., De Baets, B., 2006. A spatial approach to forest management optimization: linking GIS and multiple objective genetic algorithms. International Journal of Geographical Information Science 20(8), 917–928.

Dueck, G., 1993. New optimization heuristics: The great deluge algorithm and the record-to-record travel. Journal of Computational Physics 104(1), 86–92.

Dueck, G., Scheuer, T., 1990. Threshold accepting: A general purpose optimization algorithm appearing superior to simulated annealing. Journal of Computational Physics 90(1), 161–175.

Fotakis, D.G., 2015. Multi-objective spatial forest planning using self-organization. Ecological Informatics 29, 1–5.

Fotakis, D.G., Sidiropoulos, E., Myronidis, D., Ioannou, K., 2012. Spatial genetic algorithm for multi-objective forest planning. Forest Policy and Economics 21, 12–19.

Haveri, B.A., Carey, A.B., 2000. Forest management strategy, spatial heterogeneity, and winter birds in Washington. Wildlife Society Bulletin 28, 643–652.

Hassall and Associates, 1999. Greenhouse, carbon trading and land management, LWRRDC Occassional Paper 23/99, Land and Water Resources Research and Development Corporation, Canberra.

Hof, J.G., Joyce, L.A., 1993. A mixed integer linear programming approach for spatially optimizing wildlife and timber in managed forest ecosystems. Forest Science 39(4), 816–

834.

Hoganson, H.M., Rose, D.W., 1984. A simulation approach for optimal timber management scheduling. Forest Science 44(4), 526–538.

Kangas, J., Kangas, A., 2005. Multiple criteria decision support in forest management: the approach, methods applied, and experiences gained. Forest Ecology and Management 207(1–2), 133–143.

Kazana, V., Fawcett, R.H., Mutch, W.E.S., 2003. A decision support modelling framework for multiple use forest management: the Queen Elizabeth forest case study in Scotland. European Journal of Operational Research 148(1), 102–115.

Kirkpatrick, S., Gelatt, C. D., Vecchi, M. P., 1983. Optimization by simulated annealing. Science, 220(4598), 671–680.

Kirschbaum, M.U.F., 2000, What contribution can tree plantations make towards meeting Australia's commitments under the Kyoto Protocol?. Environmental Science and Policy 3, 83–90.

Kurttila, M., 2001. The spatial structure of forests in the optimization calculations of forest planning–a landscape ecological perspective. Forest Ecology and Management 142(1-3), 129-142.

Lauer, C., McCaulou, J. C., Sessions, J., Capalbo, S. M., 2015. Biomass supply curves for western juniper in Central Oregon, USA, under alternative business models and policy assumptions. Forest Policy and Economics 59, 75–82.

Liu, G., Han, S., Zhao, X., Nelson, J., Wang, H., Wang, W., 2006. Optimisation algorithms for spatially constrained forest planning. Ecological Modelling 194(4), 421–428.

Liu, W.-Y., Lin, C.-C., 2015. Spatial forest resource planning using a cultural algorithm with problem-specific information. Environmental Modelling & Software 71, 126–137.

Lockwood, C., Moore, T., 1993. Harvest scheduling with spatial constraints: a simulated annealing approach. Canadian Journal of Forest Research 23(3), 468–478.

Mathey, A., Krcmara, E., Taitb, D., Vertinskya, I., Innes, J., 2007. Forest planning using co-evolutionary cellular automata, Forest Ecology and Management 239(1-3), 45-56.

Murray, A. T., 1999. Spatial restrictions in harvest scheduling. Forest Science 45(1), 45–52.

Myronidis, D., Arabatzis, G., 2009. An evaluation of the Greek post fire erosion mitigation policy through spatial analysis. Polish Journal of Environmental Studies 18(5), 865–872.

Nalle, D. J., Arthur, J. L., Montgomery, C. A., 2005. Economic impacts of adjacency and green-up constraints on timber production at a landscape scale. Journal of Forest Economics 10, 189–205.

Ohman, K., Eriksson, L.O., 2002. Allowing for spatial consideration in long-term forest planning by linking linear programming with simulated annealing. Forest Ecology and Management 161(1–3), 221–230.

Ohman, K., Lamas, T., 2005. Reducing forest fragmentation in long-term forest planning by using the shape index. Forest Ecology and Management 212(1–3), 346–357.

Štefančík I., Bošeľa M., 2014. An influence of different thinning methods on qualitative wood production of European beech (Fagus sylvatica L.) on two eutrophic sites in the Western Carpathians. Journal of Forest Science 60, 406–416.

Venn, T.J., Beard, R.M., and Harrison, S.R., 2000. Modeling stand yield of non-traditional timber species under sparse data. In S. Harrison and J. Herbohn (eds), Socio-Economic Evaluation of the Potential for Australian Tree Species in the Philippines, Australian Centre for International Agricultural Research (ACIAR), Monograph 75, Canberra.

Wilkinson, C. F., Anderson, H. M., 1985. Land and resource planning in the national forest. Covelo, CA: Island Press.

Wong, J., Baker, T., Duncan, M., McGuire, D., Bulman, P., 2000. Forecasting Growth of Key Agroforestry Species in South-Eastern Australia: A Report for the RIRDC/LWRRDC/FWPRDC Joint Venture Agroforestry Program. Barton, A.C.T., Australia: RIRDC.